Synthesis and dissemination of ocean and atmosphere heat transport to the Arctic

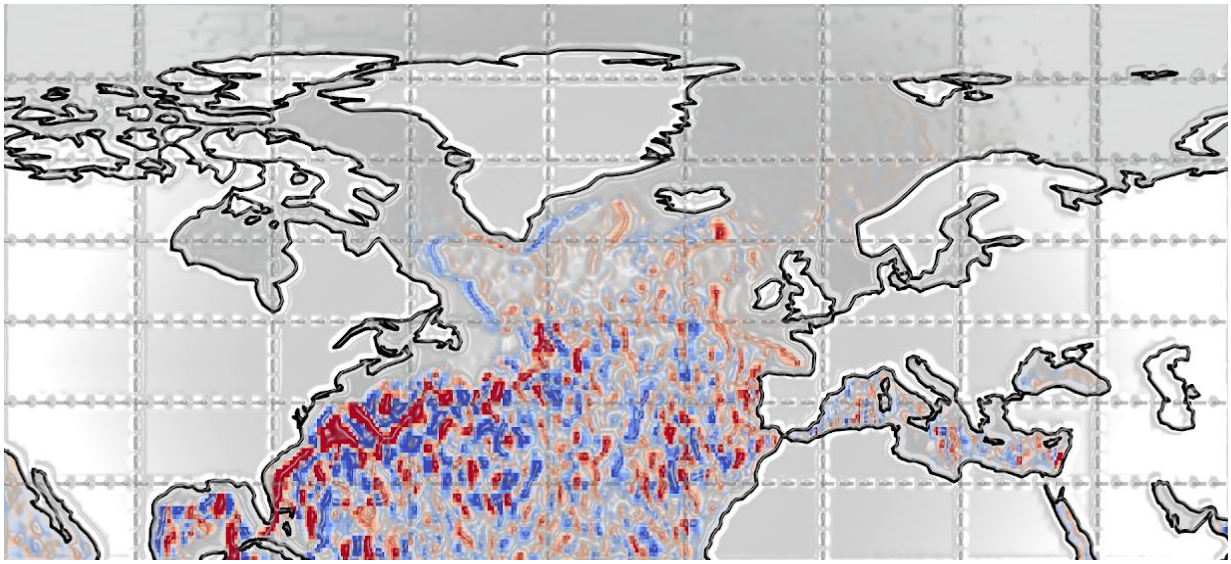

Northward Ocean Heat Transport to the Arctic. Credits: Yang Liu (NLeSC)

Blue-Action: Arctic Impact on Weather and Climate is a Research and Innovation action (RIA) funded by the Horizon 2020 Work programme topics addressed: BG-10-2016 Impact of Arctic changes on the weather and climate of the Northern Hemisphere. Start date: 1 December 2016. End date: 28 February 2021.

The Blue-Action project has received funding from the European Union's Horizon 2020 Research and Innovation Programme under Grant Agreement No 727852.

About this document

Deliverable: D2.4 Synthesis and dissemination of ocean and atmosphere heat transport to the Arctic
Work package in charge: WP2 Lower latitude drivers of Arctic changes
Actual delivery date for this deliverable: 30 November 2019
Dissemination level: The general public (PU)

Lead authors
Netherlands eScience Center (NLeSC): Yang Liu, Jisk Attema

Other contributing authors
Centre National de la Recherche Scientifique (CNRS): Guillaume Gastineau
Max Planck Institute for Meteorology (MPI-M): Daniela Matei, Rohit Ghosh
National Oceanography Centre (NOC): Ben Moat
Woods Hole Oceanographic Institution (WHOI): Young-Oh Kwon

Contributing authors from non-partner organisations
Universiteit Utrecht (UU): Wilco Hazeleger

Reviewer
Faroe Marine Research Institute (HAV): Karin Margetha Larsen

We support Blue Growth!
Visit us on: www.blue-action.eu

Follow us on Twitter: @BG10Blueaction

Access our open access documents in Zenodo:
https://www.zenodo.org/communities/blue-actionh2020

Index

Summary for publication

Meridional Energy Transport (MET), both in the atmosphere (AMET) and ocean (OMET), has significant impact on the climate in the Arctic. In this study, the quantification of atmospheric meridional energy transport (AMET) and oceanic meridional energy transport (OMET) at subpolar latitudes have been performed using six state-of-the-art reanalyses datasets (ERA-Interim, MERRA2, JRA55, ORAS4, GLORYS2V3, and SODA3). Emphasis is placed on the key processes regulating AMET and OMET from midlatitudes to the Arctic. The differences between these data sets were investigated. A forced NEMO-ORCA hindcast, two high resolution fully coupled HadGEM3-GC3.1 simulations and observations in the Atlantic from Rapid Climate Change-Meridional Overturning Circulation and Heatflux Array (RAPID ARRAY) and Overturning in the Subpolar North Atlantic Program (OSNAP) are included in the comparison. Based on the intercomparison of reanalyses data, model outputs and the observation data, sources of uncertainty are identified. The impacts of orography on the atmospheric moisture and heat transport toward the pole were studied with the IPSL-CM6 model experiments. Compensation and feedback between oceanic and atmospheric heat, moisture or energy transport impacts on the Arctic variability were checked with the CESM1 Large Ensemble simulations and the MPI-ESM-LR grand ensemble simulations (MPI-GE), which also reflect the respective role of the natural climate variability and externally forced climate change. To support our comparison of AMET and provide more insight, we further investigate AMET with multiple atmospheric model simulations (EC-Earth, HadGEM, NorSEM, WACCM6, CMCC-CM, IPSL-CM, IAP-AGCM, MPIESM) from the coordinated experiments, in collaboration with Blue-Action WP3 “Linkages of Arctic climate changes to lower latitudes”.

The main results are:

- The mean transport in all chosen atmospheric (ERA-Interim, MERRA2 and JRA55) and oceanic (ORAS4, GLORYS2V3 and SODA3) reanalyses data sets agree well, while the spatial distribution and temporal variations of AMET and OMET differ substantially among the reanalyses data sets.
- For the ocean, comparisons with observed heat transports at subtropical and subpolar Atlantic confirm that the OMET estimated from reanalyses is consistent with observations.
- The existence of sources and sinks in reanalyses data sets introduces large uncertainties in the computation of energy transport. Based on our results, it seems that AMET and OMET cannot be constrained by the available observations.
- The AMET and OMET estimated from reanalyses at large time scales should be used with great care, especially when studying variability and interactions between the Arctic and midlatitudes beyond interannual time scales.
- Strong compensation between poleward AMET and OMET was found within a fully coupled model simulation (CESM1). It also shows that OMET has significant impact on the Arctic sea ice variability and the Arctic Amplification (AA). With a grand ensemble simulation (MPI-GE), a crucial role of the significant changes in the North Atlantic sub-polar gyre strength for the increasing high latitude heat transport to the Arctic and freshening of the North Atlantic under global warming is identified.
- Generally, the chosen high resolution ocean model (NEMO ORCA) and fully coupled model (HadGEM3-GC3.1) show very good agreement with both the reanalyses and observations on OMET. There are biases between the calculated AMET from coordinated experiments and

reanalyses but the variabilities are similar. With IPSL-CM simulation, strong impact of orography on the poleward AMET is identified.

Work carried out

1. Data

Computation of AMET and OMET were performed using three atmosphere reanalyses data sets: ERA-Interim (Dee et al., 2011), MERRA2 (Gelaro et al., 2017), and JRA55 (Kobayashi et al., 2015; Harada et al., 2016) and three ocean reanalyses data sets: ORAS4 (Balmaseda et al., 2013), GLORYS2V3 (Ferry et Al., 2010 & 2012), and SODA3 (Carton et al., 2018). To avoid interpolation errors and imbalances in the mass budget introduced by regridding, the calculations are based on the data from the original model grid (Liu et al., 2019, ESD and JoClim). As a synthesis, Table 1 shows the basic specifications of the reanalyses products contained in this study.

Type	Product Name	Producer	Period	Temporal Resolution	Spatial Resolution / Grid
Atmosphere	ERA-Interim	ECMWF	1979 - 2017	6-hourly	0.75° x 0.75° x 60 levels
	MERRA2	NASA	1980 - 2017	3-hourly	0.5° x 0.625° x 72 levels
	JRA55	JMA	1979 - 2016	6-hourly	0.56° x 0.56° x 72 levels
Ocean	ORAS4	ECMWF	1979 - 2016	Monthly	1° x 1° x 42 levels
	GLORYS2V3	Mercator-Ocean	1993 - 2014	Monthly	0.25 ° x 0.25° x 75 levels
	SODA3	Univ. of Maryland	1980 - 2014	5-daily	0.25 ° x 0.25° x 50 levels

Table 1: Basic specification of reanalyses products included in this study. Note that the ocean grids are tri-polar curvilinear grids. The spatial resolutions given in the table are nominal resolutions and they vary with locations.

For the purpose of examination of the OMET calculated from reanalyses, observations of the meridional transport of mass and heat throughout the Atlantic basin are used here. We use data from the RAPID-MOCHA-WBTS program (Johns et al., 2011; McCarthy et al., 2015) and the OSNAP program (Lozier et al., 2017; Lozier et al., 2019). The RAPID MOCHA-WBTS program, which is known as RAPID ARRAY, employs a transbasin observing array along 26.5° N and it is in operation since 2004. The OMET from the RAPID ARRAY available to this study is from April 2004 to March 2016. The OSNAP program has an observing system that comprises of an integrated coast-to-coast array extending from the south eastern Labrador shelf to the southwestern tip of Greenland, and from the south eastern tip of Greenland to the Scottish shelf. So far, it provides OMET data from the full installation of the array in 2014 until the first complete data recovery in 2016, 21 months in total.

Apart from the RAPID ARRAY and OSNAP observational data, a high resolution hindcast of the NEMO ORCA ocean circulation model is also included here to provide more insights into the analysis since two of the chosen reanalyses products are also built on NEMO model (Moat et al., 2016; Marzocchi et al., 2015). This forced model simulation implements the NEMO ORCA global ocean circulation model version

3.6 (Madec, 2008). It is configured with ORCA0083 grid, which has a nominal resolution of 1/12° on 75 vertical levels. More information about this hindcast is given by Moat et al. (2016). We take monthly mean data from the hindcast, which spans from 1979 to 2012. This simulation will be referred to as OGCM simulation in the following sections.

In addition, two high resolution fully coupled simulations with HadGEM3-GC3.1 model are used to study the northward heat transport in the ocean (Roberts et. al., 2019). The results are compared with reanalyses and observations in the North Atlantic Ocean, which are again the RAPID ARRAY and OSNAP data.

In order to further evaluate the compensation and feedback between AMET and OMET, and provide more insight into the impact of MET on the Arctic variability, simulations with different numerical climate models were performed. The CESM1 LE simulation for 1950-2100 is used to investigate the role of poleward heat transports into the Arctic in Arctic warming and sea-ice melting (Fleming et al., 2019). Moreover, the IPSL-CM6 model experiments are employed to study the impacts of orography on the atmospheric moisture and heat transport toward the pole (Sandu et al., 2019). In order to distinguish the changes related to the global warming from the internal variability, a grand ensemble (GE, 100 ensemble members) of simulations with the coupled model MPI-ESM-LR is included (Maher et. al. 2019). In collaboration with WP3, comparisons of AMET between chosen reanalyses products and the coordinated experiments with nine atmospheric model simulations are also included here. The ensemble mean of control run (experiment 1, with varying sea ice and sea surface temperature) from these experiments are used for the analysis. For concision, details about the coordinated experiments in WP3 are not listed here. More information about the configuration of experiments and the outcome of the joint analysis are discussed in Deliverable 3.1. An overview of the climate models included in this study is given in Table 2.

Type	Model and simulation	Institute	Period	Spatial Resolution
Atmosphere	NorESM*	NERSC	1979 - 2015	100 km
	IPSL-CM6*	CNRS-LOCEAN	1979 - 2015	100 km
	EC-Earth3*	DMI	1979 - 2015	80 km
	CMCC-CM-HR4*	CMCC	1979 - 2015	100 km
	IAP-AGCM*	IAP-NZC	1979 - 2015	100 km
	HadGEM*	UoS	1979 - 2015	60 km
	ECHAM6.3*	MPI-M	1979 - 2015	80 km
	EC-Earth*	NLeSC	1979 - 2015	40 km
	CESM2-WACCM6 *	WHOI-NCAR	1979 - 2015	100 km
Ocean	OGCM(NEMO ORCA hindcast)	NOC	1979 - 2012	1/12 ° x 1/12 ° x 75 levels
Fully coupled model	CESM1 LE	NCAR	1950 - 2100	1° x 1° (atmosphere and ocean)
	HadGEM3-GC3.1	NOC	1950 - 2014 (historical run) 1950 - 2016 (control run)	25 km (atmosphere) and 1/12 ° x 1/12 ° (ocean)
	MPI-ESM Grand Ensemble	MPI-M	1850 - 2100	200 km (atmosphere) and 1.5 ° x 1.5 ° (ocean)

Table 2: An overview of numerical experiments with different models. (*) indicates simulations belonging to the coordinated experiments in WP3, more information about these models and simulations are shown in Deliverable 3.1)

A short summary about the contributions from each partner to every task is given in Table 3.

Contributor	Contributions
Yang Liu, Jisk Attema (NLeSC), and Wilco Hazeleger (UU)	Quantification of atmospheric and oceanic energy transport using six reanalyses datasets (ERA-Interim, MERRA2, JRA55, ORAS4, GLORYS2V3, SODA3).
Young-Oh Kwon (WHOI) and Steve Yeager (NCAR)	Investigation of the role of poleward energy transports into the Arctic in Arctic warming and sea-ice melting with NCAR CESM1 large ensemble simulation.
Guillaume Gastineau (CNRS)	Impacts of orography on the atmospheric moisture and heat transport toward the pole using IPSL-CM6 model experiments.
Ben Moat (NOC)	Comparison of oceanic energy transport from high resolution HadGEM3-GC3.1 fully coupled simulations, NEMO ORCA0083 hindcast and observations of RAPID ARRAY and OSNAP.
Daniela Matei and Rohit Ghosh (MPI-M)	Future estimate of the North Atlantic Ocean meridional heat transport in the Grand Ensemble simulations of MPI-ESM1.2
All participants in WP3 (NERSC, CNRS, DMI, CMCC, IAP-NZC, UoS, MPI-M, WHOI, NCAR)	Evaluation of atmospheric energy transport with the coordinated experiment 1 by nine atmosphere models.

Table 3: Contributions from each partner to the tasks

2. Methodology

The total energy per unit mass of air has four major components: internal energy, latent heat, geopotential energy and kinetic energy. We use an updated formulation of AMET as a combination of the divergence of dry-air enthalpy, latent heat, geopotential and kinetic energy transports, which is suggested by Mayer et al. (2017). Moreover, it should be noticed that a direct estimation of AMET based on the definitions above cannot provide a meaningful energy transport obtained from reanalyses data since reanalyses products suffer from mass inconsistency (e.g. Trenberth, 1991; Trenberth et al., 2002; Graversen et al., 2007). Spurious sinks and sources mainly come from low spatial and temporal resolution, interpolation and regridding, and data assimilation. The interpolation from original model level to pressure level can introduce considerable error to the mass budget (Trenberth et al., 2002). Therefore we prevent interpolations onto the pressure levels and use data on the native model levels with a high temporal resolution. Trenberth (1991) provided a method to correct the mass budget through the use of the continuity equation. The method assumes that the mass imbalance mainly comes from the divergent wind fields and corrects the overall mass budget by adjusting the barotropic wind. The barotropic mass budget correction includes two steps: (1) determining the mass budget imbalance and (2) correct the barotropic wind fields. More details about the implementation of barotropic mass budget correction is given by Trenberth (1991). Note that all the computations regarding barotropic mass budget correction should be performed on spectral domain via spherical harmonics (Liu et al., 2019, ESD). Differently, given the large ensemble of each experiment by nine atmosphere models in the coordinated experiments in WP3, the computation of AMET within the coordinated experiments is too expensive with direct methods. Therefore, it is computed using implied method (Liu et al., 2019, JoClim),

which takes AMET as the difference between net surface radiation and turbulent fluxes, and net radiation fluxes at the top of the atmosphere.

Unlike the atmosphere, energy transport in the ocean can be well represented by the internal energy itself (Hall and Bryden, 1982). Note that our computation of OMET suffers from mass imbalance as it is very hard to include all model components derived from oceanic reanalyses to close the budget (e.g. eddy induced velocity in ORAS4 is not available). In the ocean, with its strong boundary circulations even the smallest imbalance can lead to large errors in the heat flux. However, the barotropic correction method adopted by the atmosphere is not feasible here, as a consequence of a varying sea surface height. In oceanographic literature it is common to use a reference temperature when calculating OMET in both observations and 25 model diagnostics (e.g. Hall and Bryden, 1982; Zheng and Giese, 2009). Here we also take a reference temperature. Note that since we only have access to sub-monthly data for SODA3, the computation of OMET using monthly data in ORAS4 and GLORYS2V3 miss the heat transport by eddies.

3. Final notes

The fully coupled IPSL-CM6 simulation has not been used in the current deliverable, as originally planned in the description of the action, because of delays in the data exchanges. Instead, the analysis planned in the description of the action was successfully performed with the MPI-ESM Grand Ensemble.

Main results achieved

1. Overview of AMET and OMET

Globally, MET is driven by the unequal distribution of net solar radiation and thermal radiation. The atmosphere and oceans transport energy from regions receiving more radiation to the regions receiving less. Figure 1 gives the mean of AMET and OMET over the entire time series of every product at each latitude in the Northern Hemisphere. For the atmosphere, all three datasets agree very well. The results differ a bit in amplitude but capture similar variations along each latitude. The peak of AMET is around 41° N, after which it starts to decrease towards the north pole. In ERA-Interim and JRA55 AMET peaks at 4.45 PW at 41° N, while in MERRA2 AMET peaks at 4.5 PW at 41.5° N. These findings are consistent with previous work (e.g. Trenberth and Caron, 2001; Fasullo and Trenberth, 2008; Mayer and Haimberger, 2012 and many others).

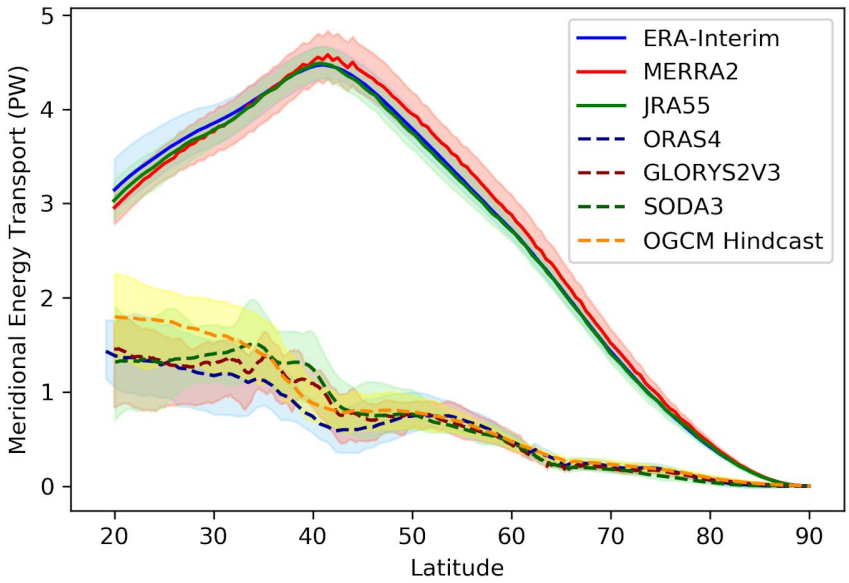

Figure 1: Mean AMET and OMET over the entire time span of each product as function of latitude in the Northern Hemisphere. AMET are illustrated with solid lines while OMET with dash lines. The shades represent the full range of MET across the entire time series at each latitude. The time span of each product used in this study is given in Table 1.

Apart from the climatology of MET, we are particularly interested in the variations across different time scales from mid-latitudes towards the Arctic. The time series of AMET, integrated zonally over 60° N, are shown in Figure 2a. The seasonal cycle is dominant in each component as expected and the phase is very similar, but differences in the amplitudes are noted. The mean AMET provided by the chosen three atmospheric reanalyses agrees well. However, their variations differ from each other. In ERA-Interim, the standard deviation (std) of AMET is 0.92 PW, while MERRA2 has a relatively large std of 0.97 PW and in JRA55 the std is 0.91 PW. Hence it can be concluded that the seasonal cycles of AMET presented by the chosen atmospheric reanalyses products are similar. After removing the seasonal cycle and applying a low pass filter, neither the amplitude nor the trend of the signals agree between the data sets (see Figure 2b). The std of the AMET anomaly in ERA-Interim is 0.02 PW, while in MERRA2 it is 0.04 PW and in JRA55 it is 0.03 PW. This implies that the variation of AMET anomalies is different in the chosen data sets. We further assess the sources of the difference in the next section.

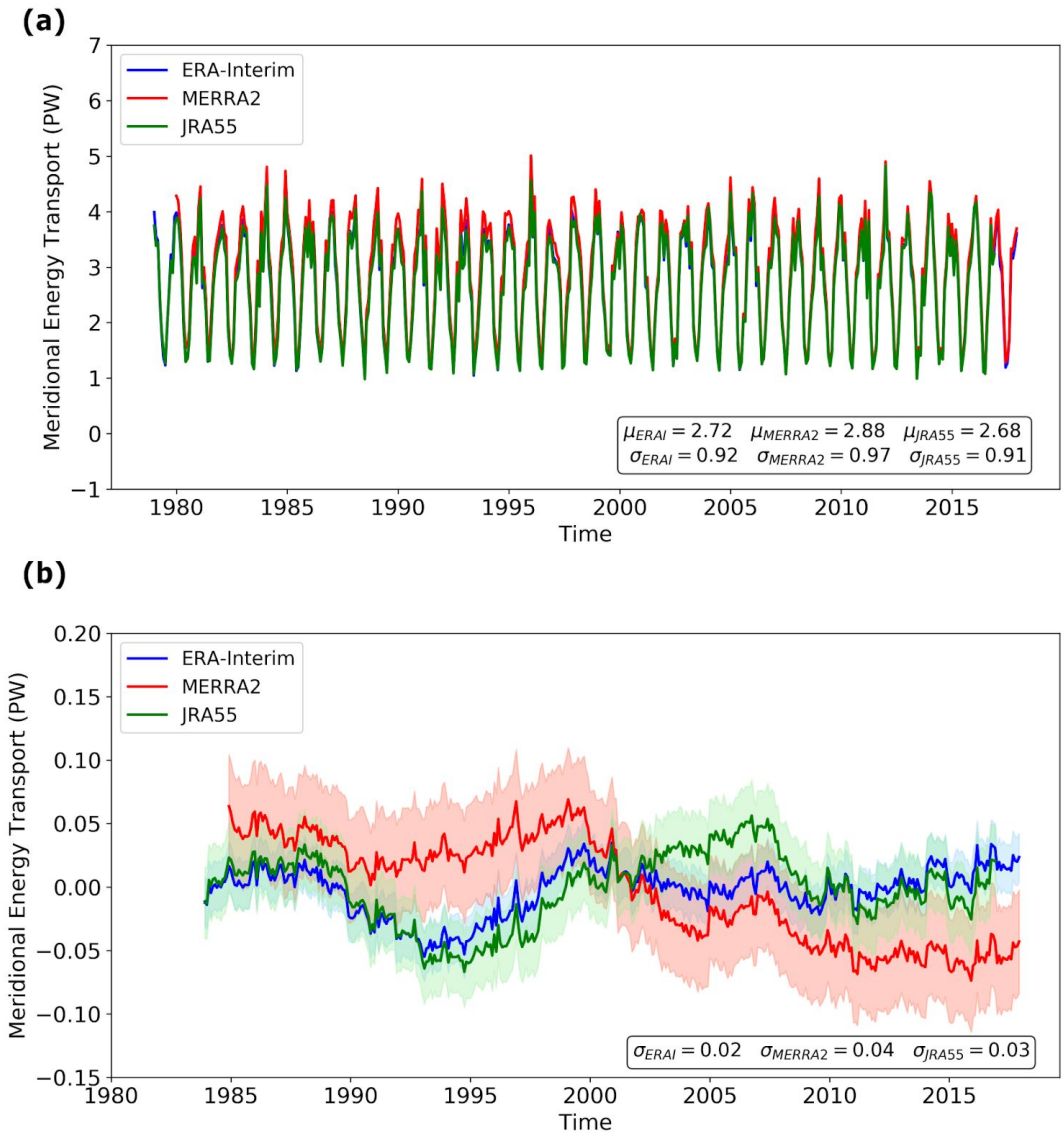

Figure 2: Time series of zonal integral of AMET at 60° N without/with low pass filter. (a) The original time series and (b) the low pass filtered time series: from ERA-Interim (blue), MERRA2 (red) and JRA55 (green). For the low pass filtered ones, we take a running mean of 5 years. The shades represent the confidence intervals with one standard deviation. σ is the standard deviation and μ is the mean of the entire time series.

For the ocean, all the reanalyses data sets agree well at almost all latitudes except for the OMET between 30° N and 40° N, where the Gulf Stream resides. The difference can be explained by the models. GLORYS2V3 and SODA3 both have been generated with eddy-permitting models while ORAS4 has not. In ORAS4, an eddy parameterization scheme from Gent-Mcwilliams (1990) is implemented. The implementation of this eddy parameterization scheme can lead to a big difference in volume transport and heat transport, compared to eddy-permitted models (Stepanov and Haines, 2014). However, in this

case the computation of OMET with ORAS4 does not include the contribution from eddy-induced velocity as the fields related to the use of eddy advection schemes are not saved by ORAS4. The eddy-permitting reanalyses with higher resolution, like GLORYS2V3 and SODA3, are capable of addressing the large-scale turbulence. It has been shown that their eddy-permitting capacity can account for the large-scale eddy variability and represent the eddy energy associated with both the Gulf Stream and the Kuroshio pathways well (Masina et al., 2017). Consequently, at the latitude of the Gulf Stream (between 30°N and 40°N), a higher spatial variability, which represents more realistic patterns of the large-scale eddy variability, is apparent in all datasets but ORAS4.

Similarly, we show the zonal integral of the OMET at 60° N in Figure 3. Differences in amplitude and trends can be observed in the unfiltered time series. The mean OMET and the std of all the OMET time series are similar (see Figure 3a). The mean OMET in ORAS4 is 0.47 PW, in GLORYS2V3 is 0.44 PW and in SODA3 is 0.46 PW. The OGCM hindcast gives a similar mean OMET of 0.47 PW. For the std of OMET, ORAS4 and the OGCM hindcast give 0.06 PW, while GLORYS2V3 and SODA3 give 0.07 PW. In terms of the difference in the OMET time series between the chosen products, it is not surprising that large differences appear after we take a running mean of 5 years when computing the OMET anomalies. However, the large variation of OMET anomalies in Figure 3b is not noticeable from their std. Given the time series of all the chosen reanalyses, ORAS4 resembles SODA3, especially after 1998, whereas, GLORYS2V3 is clearly different from ORAS4 and SODA3 from 1998 to 2006. The differences can be tracked in the time series, which reveals that the initial years of GLORYS2V3 might experience some problems. The first 10 years in GLORYS2V3 are quite suspicious because of its large deviation from the other products. Such large differences should be noticeable in the heat content changes or surface fluxes. Nevertheless, after 2007 all the reanalyses time series agree well, but the OGCM hindcast deviates from the reanalyses. It is noteworthy that the observations improve considerably around that period due to an increasing number of Argo floats in use (Riser et al., 2016). The reanalyses products used here are greatly influenced by the number of available in-situ observations. We further assess the sources of differences in the next section.

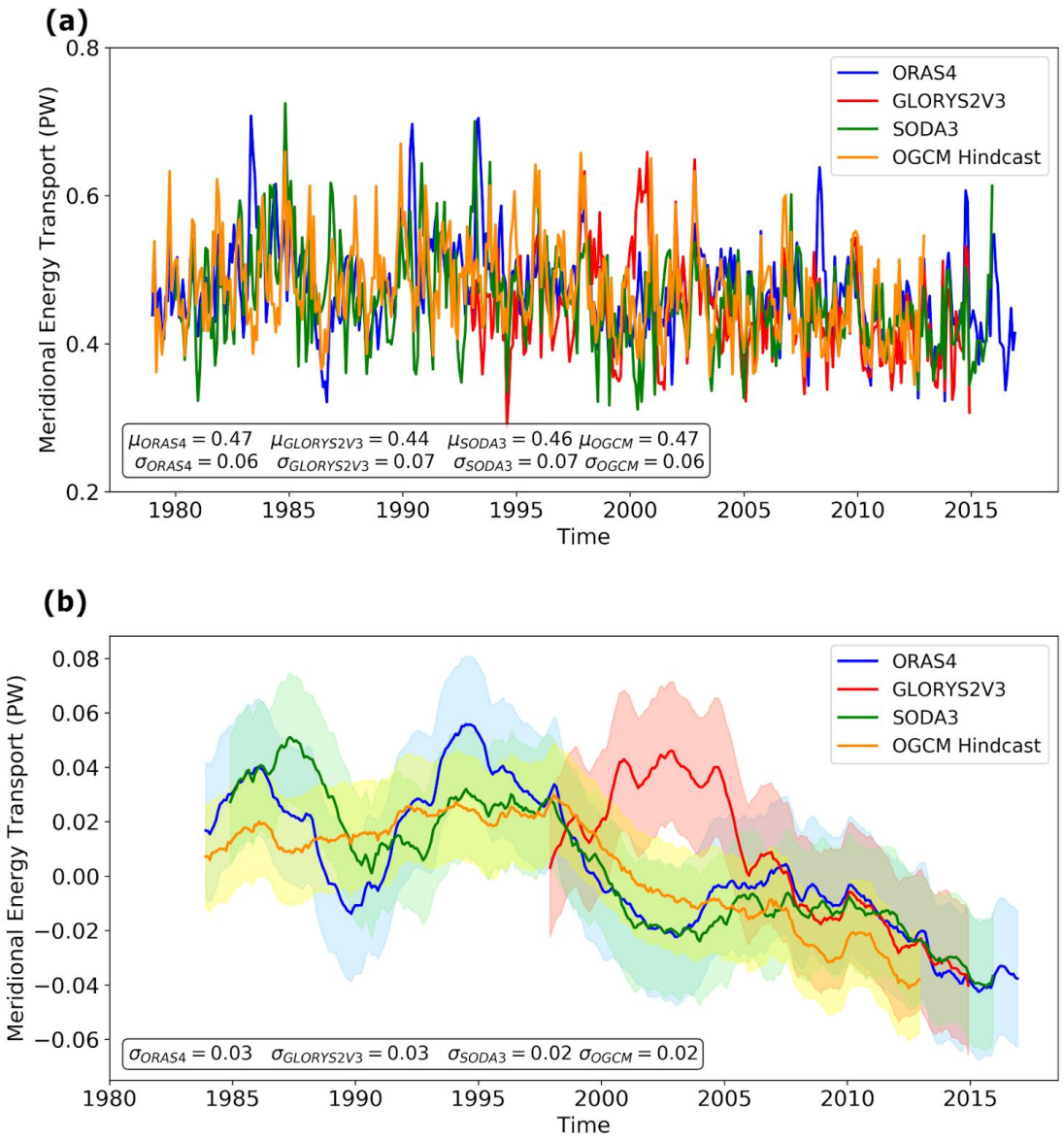

Figure 3: Time series of zonal integral of OMET at 60° N without/with low pass filter. (a) The original time series and (b) the low pass filtered time series: from ORAS4 (blue), GLORYS2v3 (red), SODA3 (green) and the OGCM hindcast (yellow). For the low pass filtered ones, we take a running mean of 5 years. The shades represent the confidence intervals with one standard deviation. σ is the standard deviation and μ is the mean of the entire time series.

2. Source of Disparity

In order to further understand the difference between the AMET estimated from each atmosphere reanalyses product, we investigate the difference between each component of AMET at 60° N estimated from ERA-Interim against those from MERRA2 and JRA55. It is noticed that the differences mainly originate from meridional temperature transport and geopotential energy transport. A simple linear regression shows the correlation between the difference of total energy transport and the

difference of meridional temperature transport, taking ERA-Interim and MERRA2, is 0.55, while for ERA-Interim and JRA55 that is very small. In addition, the correlation between the difference of total energy transport and the difference of geopotential energy transport, for ERA-interim and MERRA2 is 0.56 and for ERA-Interim and JRA55 that is 0.60. For the other components, the correlations between them and the total difference are neglectable. The results are all obtained with a confidence interval over 95%. This is generally the case as large differences in temperature transport between reanalyses products are found at all latitudes (not shown). Such differences are consistent with the fact that the temperature transport and geopotential energy transport have larger contribution to the total AMET. Note that the differences of each AMET component between every two products are of the same order of magnitude as the absolute values of that component. Besides, the latent heat transport agrees well between all the chosen atmospheric products, in terms of the mean and anomalies (Liu et al., 2019, ESD). A similar result was found by Dufour et al. (2016) in their study using more reanalyses data sets.

In order to know the relative contribution of each field to the difference of the total AMET among the chosen reanalyses, a direct comparison of the vertical profile of temperature and meridional velocity fields between ERA-Interim and MERRA2 is presented in Figure 4, as an example. We take the monthly mean temperature and velocity fields of ERA-Interim and MERRA2 from 1994 to 1998, in which the biggest difference was observed (Figure 2, taking into account the running mean of 5 years). For the sake of a point-wise comparison, the fields from MERRA2 are interpolated onto the vertical grid of ERA-Interim. This shows that these two reanalyses products differ substantially regarding each variable field (Figure 4a and b). Big differences in temperature reside mostly at the tropopause, while large differences in meridional wind component are distributed over the entire vertical profile of the atmosphere. Such differences in both fields are expected to be responsible for the difference in temperature transport. Large differences are found in geopotential height fields, too (Liu et al., 2019, ESD). It should be noted that this comparison is carried out on pressure levels and the mass conservation is not ensured. Therefore, it can only provide insight qualitatively and a quantitative contribution of the difference in each single field to the temperature transport cannot be identified here.

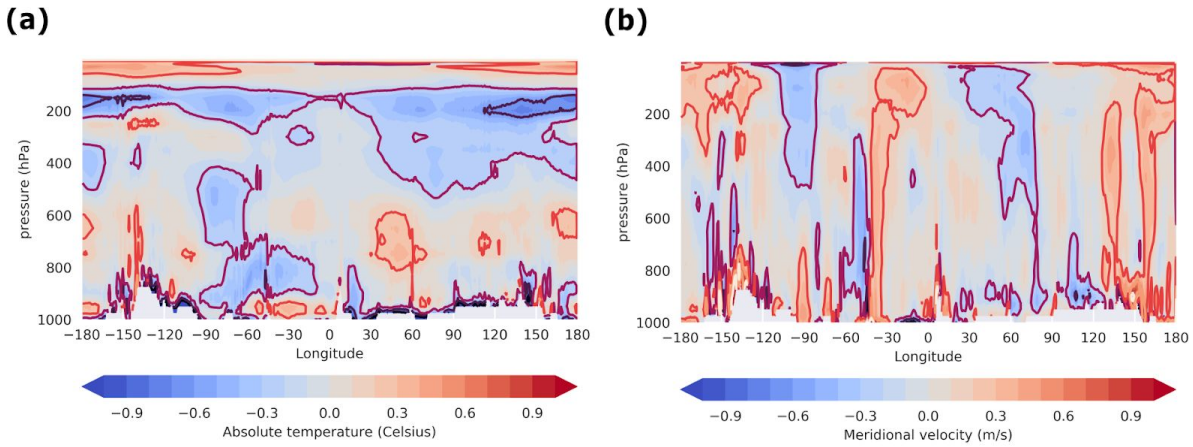

Figure 4: Difference in temperature, meridional wind velocity and temperature transport between MERRA2 and ERA-Interim at 60° N. The vertical profile of (a) temperature difference and (b) meridional wind velocity difference are calculated from the climatology of each fields from 1994 to 1998.

Differences between every two chosen atmospheric products are found at nearly each pressure level. Given the data available, this analysis is not sufficient to explain conclusively where the uncertainty mainly comes from in terms of the dynamics and physics in the atmosphere model and data assimilation system. We do find that uncertainties as indicated by the spread between the datasets, in both the temperature and meridional velocity fields, are too large to constrain the AMET. Hence studies on low frequency variability of energy transports and associated variables, should be interpreted with care as the reanalyses products differ substantially and we cannot make a priori judge how close they are to actual energy transports since independent direct observations are not available.

For the ocean, fortunately observations of OMET in the Atlantic Ocean are available. First, OMET estimated from ORAS4, GLORYS2V3, SODA3, and the OGCM (NEMO) hindcast are evaluated against OMET measured at 26.5° N. Given in Figure 5, the inter-comparison shows that the reanalyses products capture roughly the mean amplitude of the OMET. Some large events are captured as well, such as the strong weakening in 2009. Statistically, the mean OMET provided by RAPID ARRAY is 1.21 ± 0.27PW. It is higher than all the chosen products here. The mean OMET in ORAS4 is 0.66 ± 0.27PW, in GLORYS2V3 it is 0.89 ±0.52PW, in SODA3 it is 0.81 ± 0.52PW and in OGCM hindcast is 1.05 ± 0.21PW. This means that all chosen reanalyses products underestimate the mean OMET at 26.5° N in the Atlantic basin. Of all products, ORAS4 has the largest bias. The std of OMET given by ORAS4 is the same as that from RAPID ARRAY, while both in GLORYS2V3 and SODA3 we find a higher std of OMET. The OGCM hindcast has a relatively small OMET std of 0.21 PW. In terms of the correlation and standard deviation, ORAS4 and the OGCM hindcast agree well with observations. It is noteworthy that NEMO does not assimilate ocean data. The simulation is only constrained by the surface fluxes. To conclude, the heat transport at 26.5° N is too low in these reanalyses products.

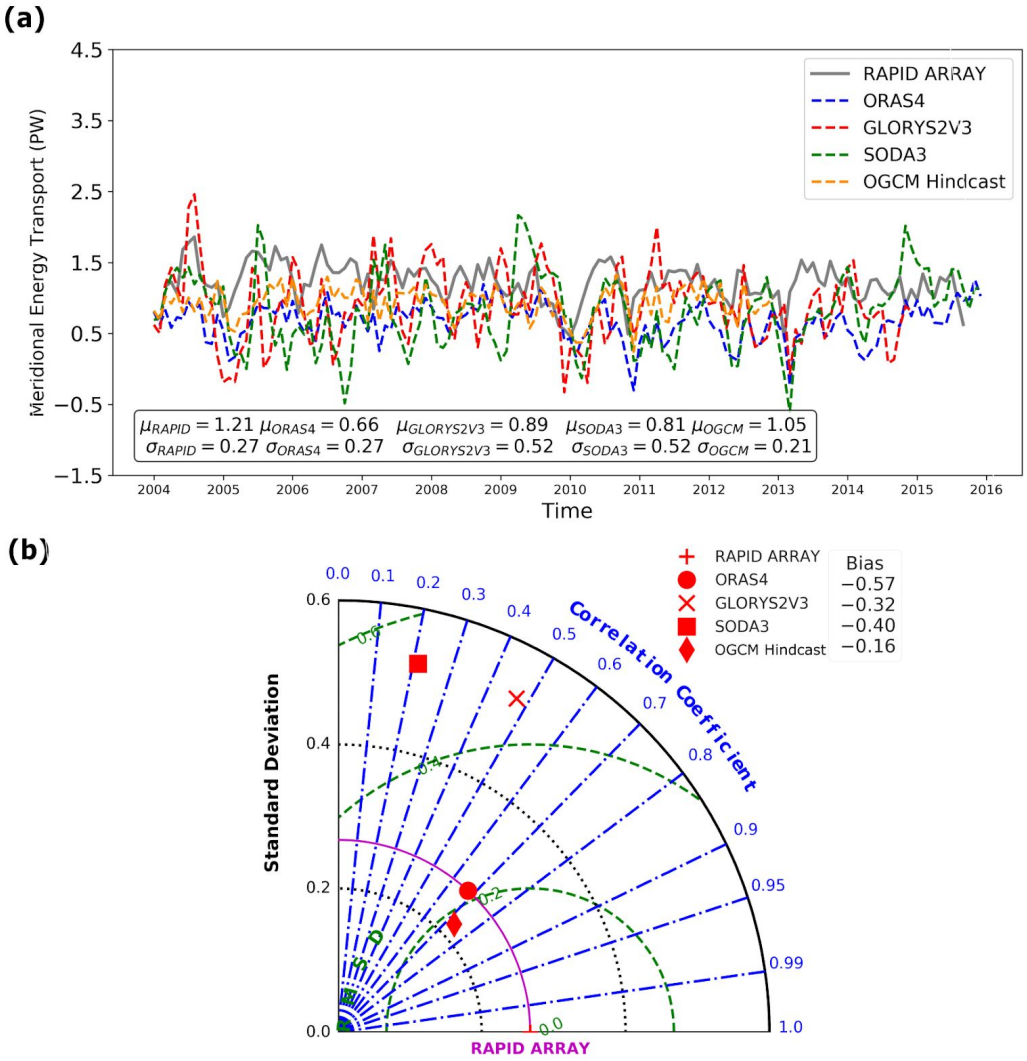

Figure 5: OMET estimated from ORAS4 (blue), GLORYS2V3 (red), SODA3 (green) and the OGCM hindcast (orange) compared to the RAPID ARRAY observation (grey) at 26.5° N across the Atlantic basin. The time series of OMET is presented in (a). The statistical properties are shown in (b) Taylor Diagram, including bias, correlation (blue), standard deviation (black) and root mean square deviation (green). σ is the standard deviation and μ is the mean of the entire time series.

Moreover, the comparison of time series in the chosen reanalyses and OSNAP observations is given in Figure 6. Due to the limited length of the OMET time series, only ORAS4 and SODA3 are included in the comparison. It can be noticed that the OMET given by ORAS4 is quite comparable to that in OSNAP in terms of the amplitude and variations. For most of the time within the observation period, OMET in ORAS4 falls into the range of the OSNAP observation including the uncertainty margins. The mean of OMET in ORAS4 is 0.37 ± 0.08PW, which is quite similar to the mean OMET 0.45 ± 0.07PW of OSNAP. However, OMET in SODA3 has a larger mean and standard deviation than the OMET in OSNAP and thus deviates from the observation.

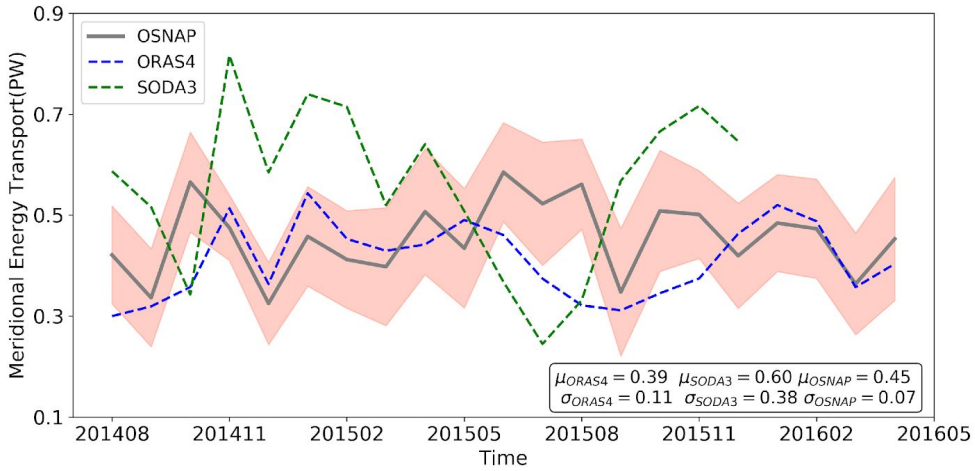

Figure 6: OMET estimated from ORAS4 (blue), SODA3 (green) and compared to the OSNAP observation (gray) at subpolar Atlantic basin. The range of uncertainty from OSNAP observation is marked by the red shade. σ is the standard deviation and μ is the mean of the entire time series.

Just as in the atmosphere we would like to study the temperature and meridional current velocity contributions to the ocean heat transport to identify the sources of the difference between products. However, due to the nature of curvilinear grid, the comparison of local fields after interpolation is not trustworthy. To get further insight, we calculate the ocean heat content (OHC), since the convergence of the heat transports are likely related to OHC change. A full budget analysis was not feasible as most datasets did not include the surface fluxes. Figure 7 illustrates the OHC (Figure 7a) and the OHC anomalies (Figure 7b) quantified from ORAS4, GLORYS2V3, SODA3 and the OGCM hindcast. It depicts the OHC integrated in the polar cap (from 60° N to 90° N) over all depths. The mean OHC in ORAS4 is 4.48 ± 0.78 x 10^{22}J, in GLORYS2V3 is 4.23 ± 0.59 x 10^{22}J and in SODA3 is 3.79 ± 0.93 x 10^{22}J, while the OGCM hindcast shows a much larger mean OHC of 7.85 ± 0.58 x 10^{22}J. The variations are similar between chosen products. Regarding the OHC anomalies in Figure 7b, an increasing trend of OHC anomalies in the polar cap is captured by each product. However, the variations are different and these are reflected in the std of OHC anomalies time series. To conclude, for the OHC there are large difference between chosen products while their variations agree very well. Since OHC is a function of temperature fields only, this can imply that temperature profiles are different among all the chosen ocean reanalyses data sets. The chosen reanalyses data sets agree well. The differences of OHC between chosen products are partially consistent with the differences that we found for OMET. However, the OHC anomalies agree better with each other than the absolute OHC, which indicates that the trend of OHC is captured in a similar way among all the ocean reanalyses products.

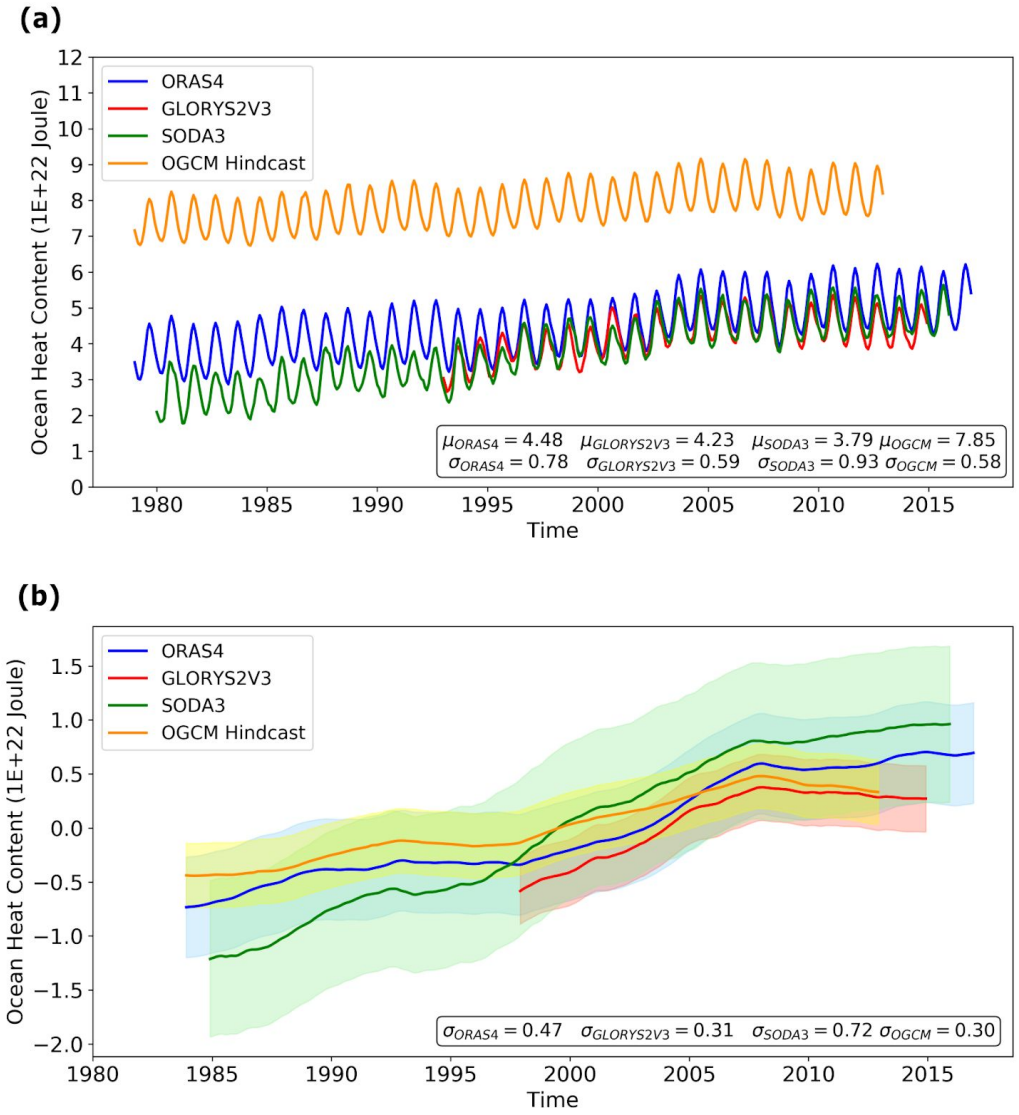

Figure 7: Time series of (a) ocean heat content (OHC) and (b) OHC anomalies with a low pass filter inside the polar cap. The OHC is integrated from surface to the bottom between 60° N and 90° N. It is estimated from ORAS4 (blue), GLORYS2V3 (red), SODA3 (green) and the OGCM hindcast (yellow). The shades represent the confidence intervals with one standard deviation. σ is the standard deviation and μ is the mean of the entire time series.

3. MET in Numerical Climate Models

In previous sections it is found that MET of different reanalyses products at subpolar and subtropical latitudes differ substantially from each other. In order to further evaluate the compensation and feedback between AMET and OMET and provide more insight into the influence of MET on the Arctic, we investigate the key processes regulating AMET and OMET in numerical climate models.

3.1 Compensation and Feedback between AMET and OMET

The CESM1 Large Ensemble simulation for 1950-2100 is used to investigate the role of poleward heat transports into the Arctic in Arctic warming and sea-ice melting (Fleming et al., 2019). We found a large increase toward the end of the 21st century in ocean heat transport (OMET) into the Arctic, with the largest increase in OMET through the Barents Sea Opening (Fig. 8b). While the Atlantic meridional overturning circulation (AMOC) transport is projected to decrease in all 40 members, the ocean volume transport into the Arctic is projected to be stable in 1950-2100 (Fig. 8c). Thus, the increasing OMET can be attributed primarily to the warming in the subarctic North Atlantic. In addition to the ensemble mean trend, the inter-ensemble spread suggest the OMET increase is significantly correlated with both Arctic amplification and sea-ice reduction (Fig. 8d). When the sum of OMET through the five Arctic straits is compared with more commonly used northward OMET at a fixed latitude, we found the latter approach is highly sensitive to the choice of latitude (Fig. 8e). We also examined the atmospheric heat transport (AMET) into the Arctic. The total AMET shows a decreasing trend (Fig. 8f) on the same order as the increases in OMET (Fig. 8e), thus the two are overall compensated. The total decreasing trend in AMET results from a difference between increasing dry statistic energy transport and a larger decrease in latent energy transport. However, unlike the OMET, the ensemble spread in AMET changes does not exhibit any significant correlation with the Arctic amplification or sea-ice change.

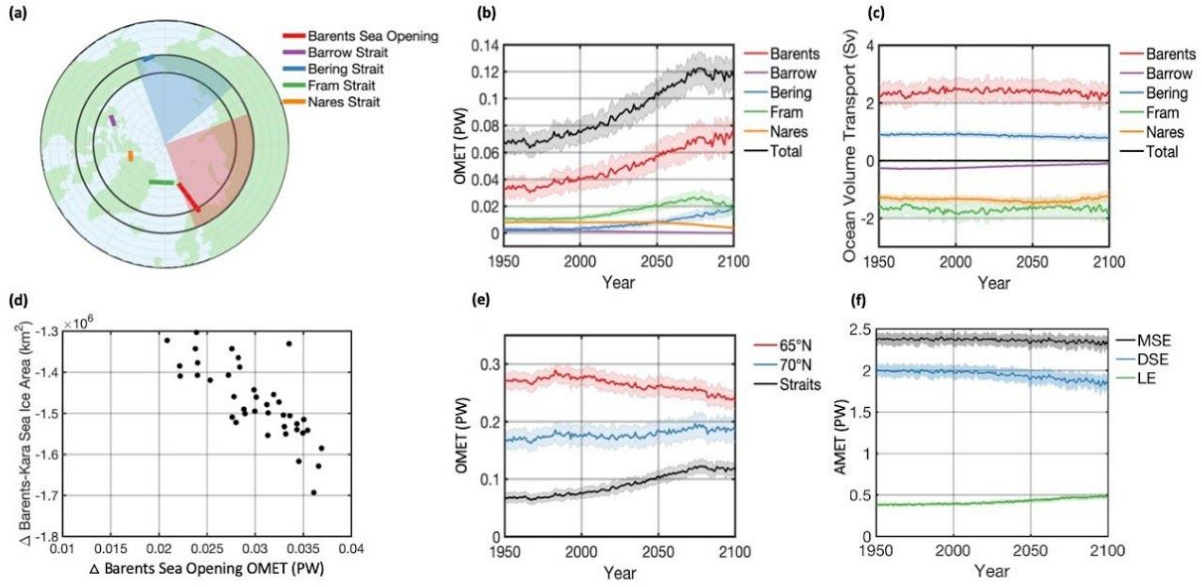

Figure 8: The OMET and AMET into Arctic in the CESM1 Large Ensemble. (a) The locations of the Arctic sections, which are the pathways of OMET into Arctic. Also shown are the 65th and 70th parallels north shown in black, the Barents-Kara Seas sector shaded in red, and the Chukchi-East Siberian Seas sector shaded in blue. (b) The OMET into the Arctic with the total (black) as well as the contributions from each of the five Arctic straits (colors). (c) The corresponding ocean volume transports (note that the total and the standard deviations are nearly 0). (d) Scatter plot between the changes in the total sea-ice area in the Barents-Kara Seas sector vs. the changes in Barents Sea Opening OMET. The changes are calculated between 2001–2020 and 2081–2100. (e) The OMET at 65°N (red), 70°N (blue), and sum across the five Arctic straits (black). (f) The northward AMET across 65°N. The total moist static energy transport (MSE, black) is decomposed into the transport of dry static energy (DSE, blue) and latent

energy (LE, green). The thick lines represent the ensemble mean and the shadings represents one standard deviation of the ensemble spread.

3.2 Impacts of Orography on AMET

The impacts of orography on the large-scale atmospheric circulation account for some of the largest errors in numerical weather prediction or climate models (Sandu et al., 2019). We used the IPSL-CM6 model experiments to study the impacts of orography on the atmospheric moisture and heat transport toward the pole. We focus on the unresolved orography in IPSL-CM6 where the sub-grid scale orography (SSO) effect is calculated applying a drag force, opposed to the local wind following the scheme of Lott and Miller (1997), and applying a lift force, perpendicular to the local wind as detailed in Lott (1998). We performed atmosphere-only experiments using the atmospheric component of IPSL-CM6A-LR (i.e. LMDZORv6) and climatological observed SST calculated over 1979-2014. These simulations last 30-yr. We also performed coupled experiments, using two ensembles of 5 members of the IPSL-CM6A-LR atmosphere-ocean general circulation model, with duration of 80-yr. In the coupled and atmosphere only cases, we use both decreased drag force and increased lift force in the experiments, referred to as Coupled-Orog and Atm-Orog. These simulations are compared to corresponding control simulation ensembles, where the SSO is not modified, referred to as Coupled-Ref and Atm-Ref.

The main impact of decreasing drag and increasing lift for the surface temperature is shown in Fig. 9a. The SSO changes applied warms the surface temperature over land and Arctic in the atmosphere-only experiments. We also obtain in Atm-Orog an increase in the high-frequency variance of the geopotential height. The warming and the intensified storm tracks are consistent with the intensified eddy-driven jet and larger baroclinic instabilities acting to intensify the AMET (Fig. 9b) between 35°N and 60°N. This warming is only simulated in winter (DJFM). The coupled experiments reveal even larger impacts in the Northern Hemisphere, as the warming induced by SSO is amplified by a melting of the Arctic sea-ice (not shown). The melting of the sea is explained by the weaker ice growth in winter. In the coupled experiments, an increasing AMOC (see Fig. 9c) is simulated leading an overall increased OMET in the Northern Hemisphere. The AMET changes obtained in the coupled case are much larger and opposite than those simulated in the atmospheric-only simulations. This illustrates that the AMET changes, in this case, are mostly modified by the Arctic sea-ice melting and the polar amplification of the warming.

This work shows that the SSO effect can control the amount of Arctic sea-ice in a climate model. It could lead to a different partitioning of the oceanic and atmospheric energy transport. Using observations can be then used to improve the tuning of the SSO in climate models.

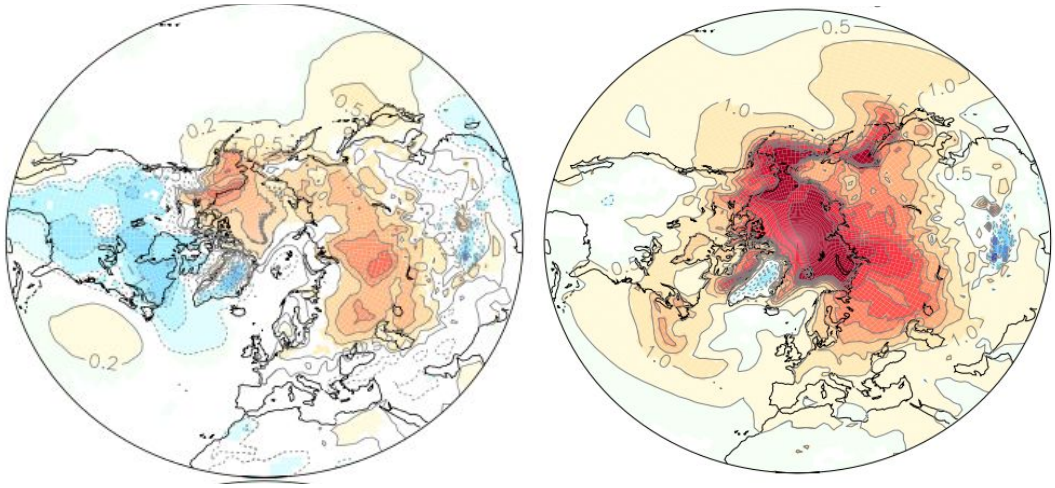

Figure 9a: Difference of 2m temperature (in K) in DJFM for (Left) Atm-Orog minus Atm-Ref, (Right) Coupled-Orog minus Coupled-ref. The contour interval is 0.5K in both panels. To provide more details of the anomalies, the 0.2K contour interval was added. Colours are masked if the level of confidence is below 90%.

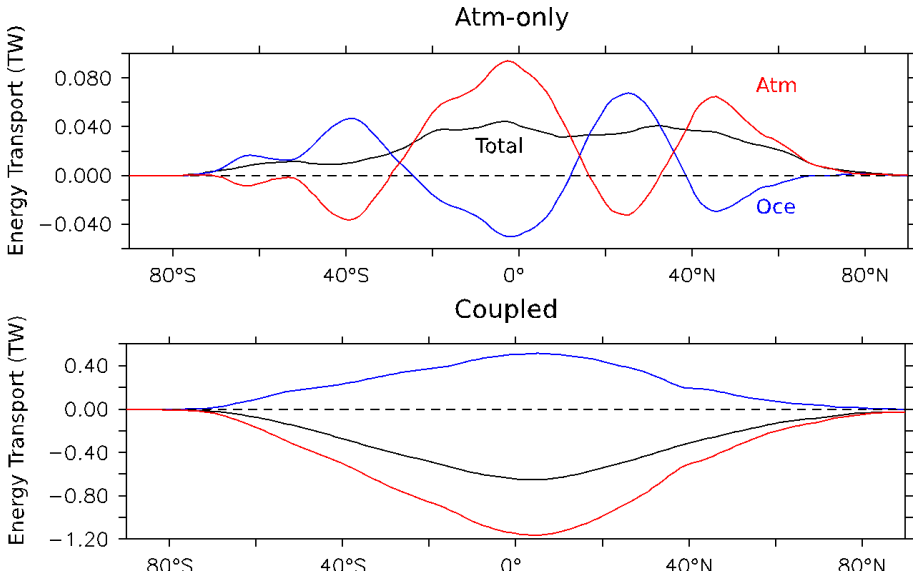

Figure 9b: Difference of (black) total, (red) atmospheric and (blue) oceanic energy transport (in K) for (Top) Atm-Orog minus Atm-Ref, (Bottom) Coupled-Orog minus Coupled-ref.

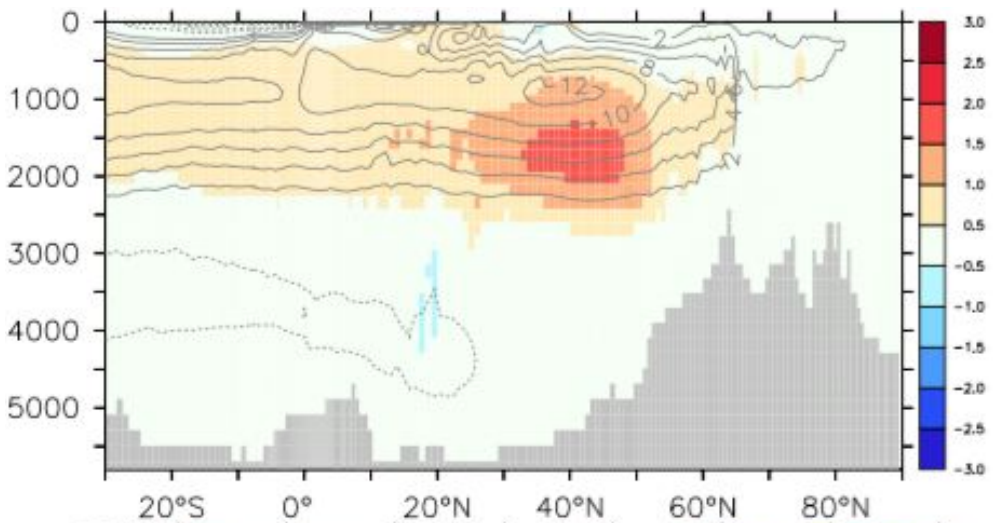

Figure 9c: Difference of Atlantic meridional overturning stream function, in Sv, for Coupled-Orog minus Coupled-ref.

3.3 OMET in Fully Coupled Climate Model Simulations

Two high resolution fully coupled simulations with HadGEM and NEMO are included to provide more information about the variation of OMET in the North Atlantic Ocean. OMET from model simulations are compared to the RAPID ARRAY and OSNAP observations, as shown in Figure 10. The mean OMET provided by HadGEM3-GC3.1 simulations are similar to the observations, within historical run is 1.18 ± 0.19PW and within control run is 1.29 ± 0.23PW. It is found that both the control run and historical run can provide OMET similar to the RAPID ARRAY observation, in terms of the mean and the variability. However, RAPID ARRAY has a slightly larger standard deviation. Besides, the OMET time series from the control run is also comparable to observed time series from OSNAP (see Figure 11), there is a bias between the OMET series from control run and OSNAP, though. Consequently, both the historical and the control runs are able to generate OMET that is comparable to the observations in the North Atlantic Ocean.

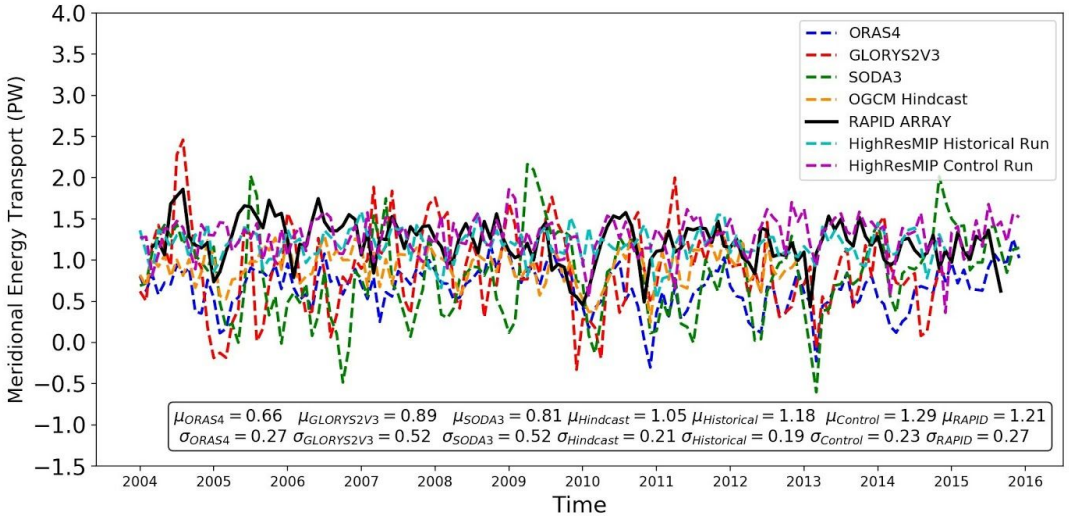

Figure 10: Same as Figure 5 but including historical (cyan) and control (magenta) runs of fully coupled simulations with HadGEM3-GC3.1 compared to the RAPID ARRAY observation (grey) at 26.5° N across the Atlantic basin.

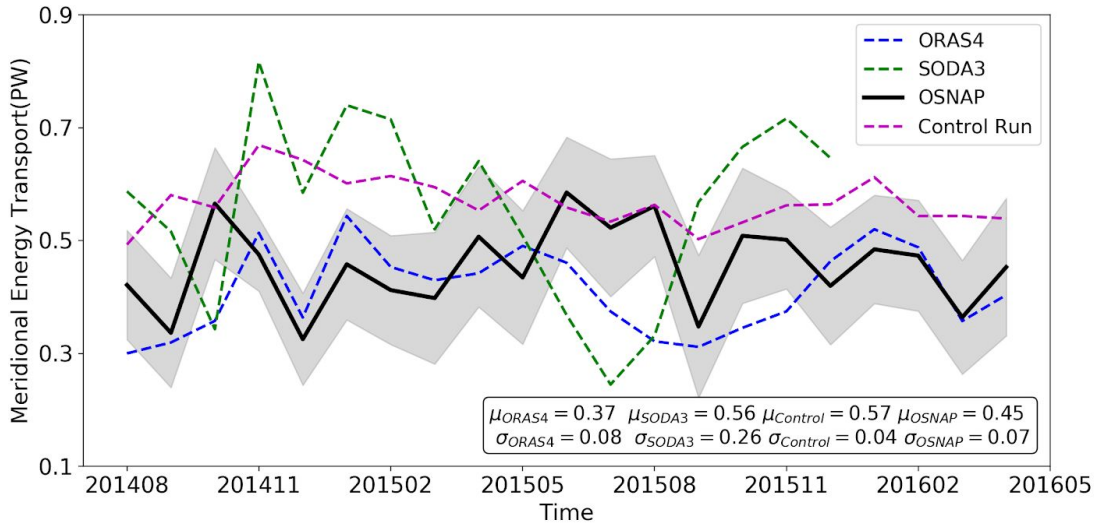

Figure 11: Same as Figure 6 but including control (magenta) runs of fully coupled simulations with HadGEM3-GC3.1 compared to the OSNAP observation (black) at subpolar Atlantic basin. The grey shading indicates the uncertainty in the observation.

Observational estimates of the overturning circulation and heat transports in the North Atlantic in the framework of the RAPID project have shown considerable interannual to multi-decadal scale variations. Therefore, the detection of a possible anthropogenic trend is hampered by the uncertainty from the

internal variability. With an aim to provide an estimate of the robust changes in the future basin wide OMET in the North Atlantic Ocean in response to global warming to help set priorities for the future ocean observing system, a grand ensemble (GE, 100 ensemble members) of simulations with the coupled model MPI-ESM-LR is used to distinguish the changes related to global warming from the internal variability (Maher et. al. 2019). The simulations include the historical period (1850-2005) continued to the 21st century scenarios (2006-2099) and also a more idealised 1%CO^2-increase-per-year experiment.

Compared to the beginning of the historical period, the ensemble mean OMET in the North Atlantic Ocean shows considerable decrease in the lower latitudes and increase in the higher latitudes towards Arctic from the start of the 21st Century (Fig 12a), similar to what is found in the previous studies (Jungclaus et. al. 2014). The anomalies seem to intensify in the coming decades. The decrease in the heat transport in the lower latitudes (0-40N) is related to the OMET changes from the weakening of the meridional overturning circulation (MOC, Fig 12b). The increase in the OMET over the Atlantic towards Arctic in the higher latitudes is partly contributed by both MOC and gyre and driven by the increase in subpolar gyre strength (Ghosh et.al., submitted), which drives more heat towards Arctic (Fig 12c). The recent observed SPG strengthening signature and its underlying dynamics are similar to the anthropogenically forced SPG strengthening in MPI-GE (shown in Ghosh et.al., submitted).

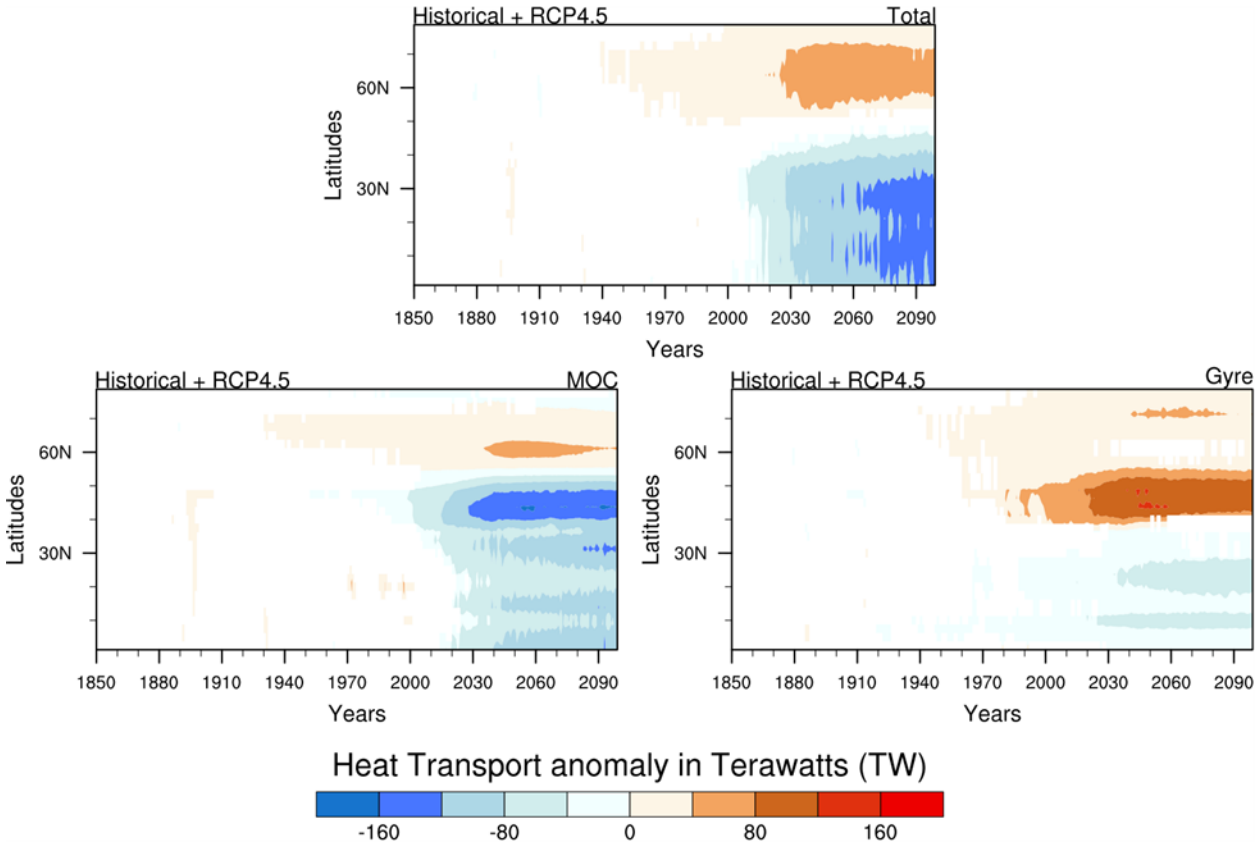

Figure 12: The difference of the ensemble mean in the a) total b) MOC and c) gyre components of the North Atlantic basin wide OMET from the respective ensemble mean of the heat transport in 1850 to

1860, over 0-80N in Terra Watts (TW) in the GE historical simulations continued to the RCP 4.5 scenarios. The negative (positive) values denote the decrease (increase) in mean of the heat transport.

Using a large ensemble with 100 members helps us to most efficiently understand the changes in the internal variability, represented by ensemble standard deviation, under global warming. The results reveal that the internal variability in the heat transport decreases in the lower to mid-latitudes in the 21st Century with the most intense decrease in the intergyre region (40-50N) and there is a slight increase in the internal variability over the northern most latitudes towards Arctic (Fig 13a). The decrease in variability over the inter-gyre region is contributed by both MOC and the gyre (Fig 13b,c). This weakening variability, in associated with a prominent change in the mean state (Fig 12), indicates an enhanced chance of detecting the anthropogenic changes in the total heat transport in the coming decades over this region. Further research is in progress to determine that, how long an observational record we might need to distinguish the anthropogenic signature in the heat transport changes from the internal variability.

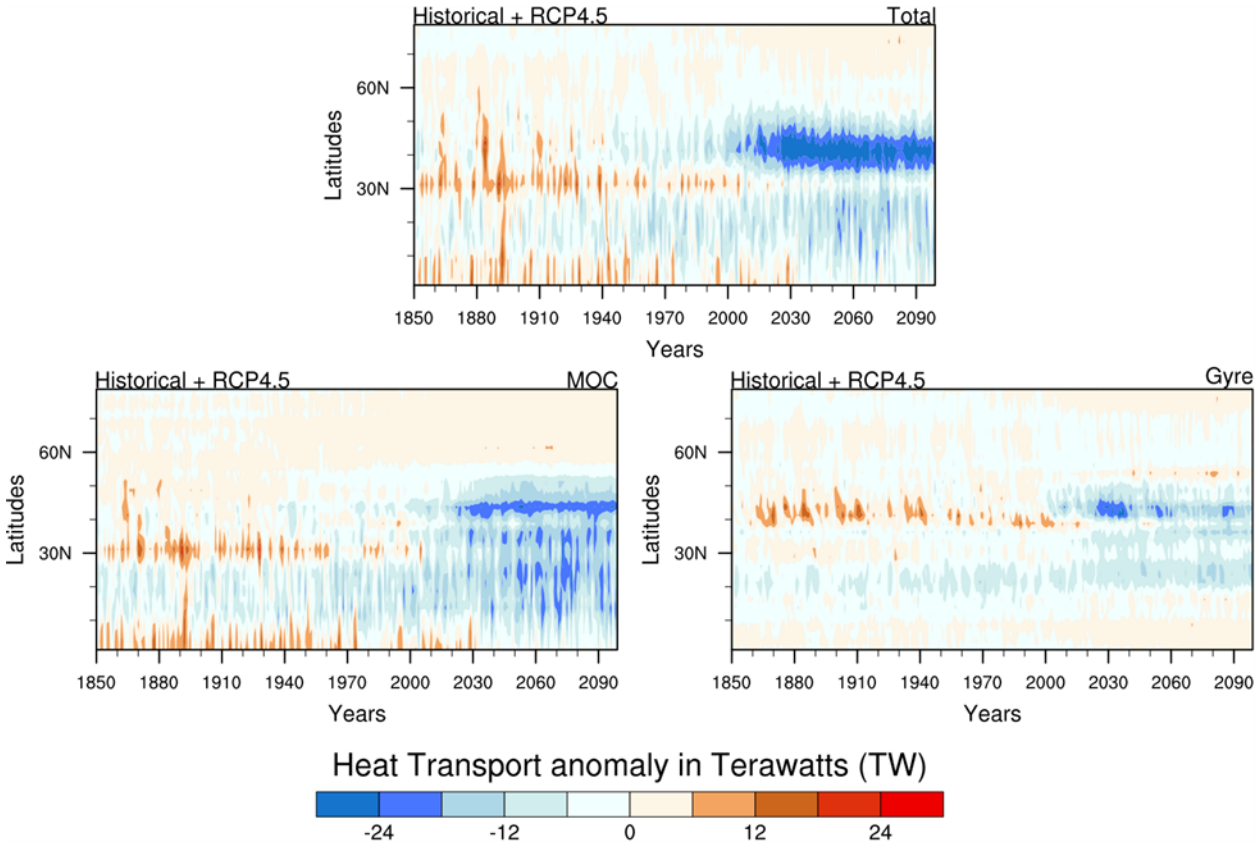

Figure 13: The difference of the ensemble standard deviation in the a) total b) MOC and c) gyre components of the North Atlantic basin wide OMET from the respective ensemble standard deviations of the heat transport in 1850 over 0-80N in Terra Watts (TW) in the GE historical simulations continued to the RCP 4.5 scenarios. The negative (positive) values denote the decrease (increase) in variability of the heat transport.

The research has shown a crucial role of the significant changes in the North Atlantic sub-polar gyre strength for the increasing high latitude heat transport to the Arctic and freshening of the North Atlantic under global warming (Ghosh et.al., submitted). For the future work, emphasis is placed on finding the future estimates of the heat transport contribution especially through the Greenland-Scotland ridge, which is one of the key regions for observational network.

3.4 AMET in Atmospheric Model Simulations

In collaboration with WP3, the analysis is extended with AMET computed from the coordinated experiments by the nine atmosphere-only models to provide more insight into the energy transport variability in the atmosphere. The mean AMET in the Northern Hemisphere at each latitude from chosen reanalyses products and the coordinated experiment 1 is shown in Figure 14. It is found that only the EC-Earth simulation with high resolution (40 km) and IAP-AGCM simulation are comparable to the reanalyses at almost all the latitudes. There are large bias in AMET between the rest of the models and reanalyses, while the variations of AMET as a function of latitudes are very similar among all the reanalyses and the coordinated experiments. We further examine the low frequency AMET anomalies in these models. The time series of zonal integral of AMET anomalies at 60° N with low pass filter from each reanalyses product and atmosphere model simulation from the coordinated experiments are shown in Figure 15. The results given by atmosphere models from the coordinated experiments agree relatively well. However, they are very different from ERA-Interim and JRA55, in terms of the magnitude and variability. The variations of the low frequency signals of AMET anomalies from atmosphere models are similar to that from MERRA2, despite of the difference in magnitudes. Given the difference of AMET anomalies at large time scales in reanalyses and the complexity of atmosphere models, it is not surprising to find such difference in low frequency signals of AMET. In summary, most of the atmosphere models tend to overestimate the mean AMET in the North Hemisphere. The AMET anomalies at large time scales are different from reanalyses but the differences are acceptable in terms of the magnitude and variability.

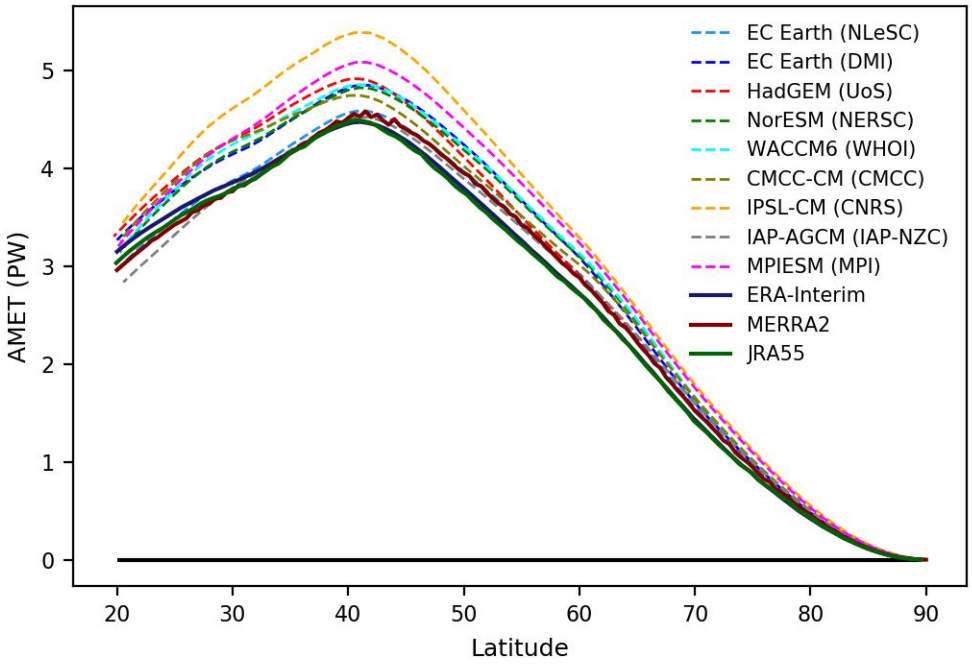

Figure 14: Mean AMET over the entire time span of each reanalyses product and atmosphere model simulation from the coordinated experiments as a function of latitude in the Northern Hemisphere. AMET from reanalyses are illustrated with solid lines while those given by models with dash lines. The time span of each reanalyses product and model simulation used in this study is given in Table 1 and 2.

More details about the coordinated experiments and an inter-comparison of AMET from each experiment can be found in Deliverable D3.1[1].

[1] D3.1: http://www.blue-action.eu/index.php?id=4122

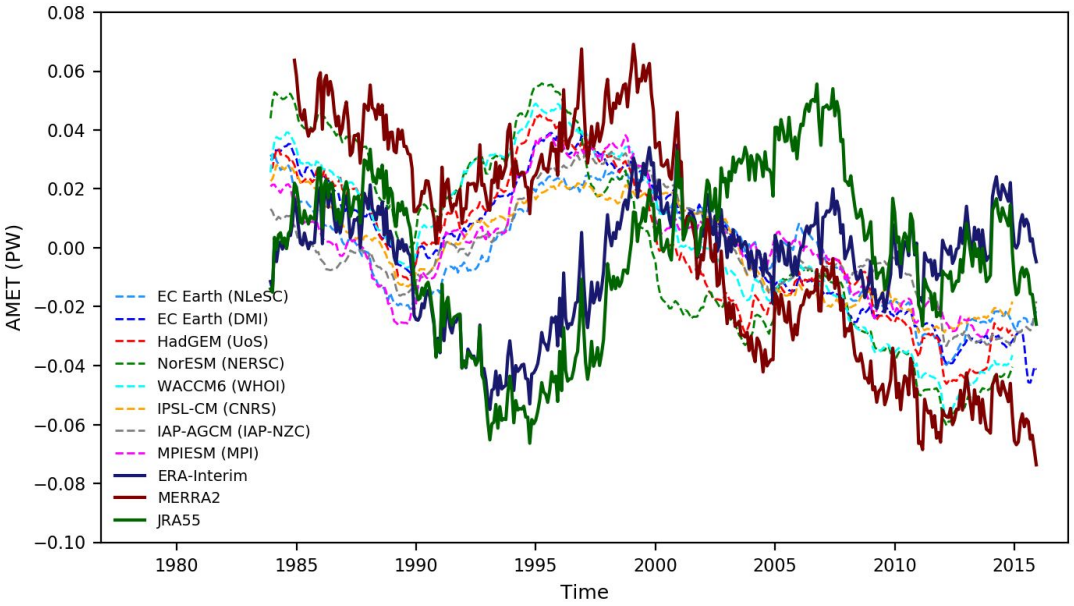

Figure 15: Time series of zonal integral of AMET anomalies at 60° N with low pass filter from each reanalyses product and atmosphere model simulation from the coordinated experiments. For the low pass filtered ones, we take a running mean of 5 years.

Progress beyond the state of the art

The study is motivated by previous studies with reanalyses data, where generally only one reanalyses data set is considered, and which includes mostly only oceanic or atmospheric analysis. For the first time, the quantification and inter-comparison of AMET and OMET variability at subpolar latitudes were performed with multiple the state of the art atmospheric and oceanic reanalyses data sets, and many advanced atmosphere and ocean models. Serving as a guideline for the evaluation of energy transports using reanalyses, this study gives a better scope of the reanalyses products with respect to the energy transport and provides more insights into the usage of reanalyses in diagnostics. It highlights that the reanalyses are very useful for assessing the quality of products and further underlines the importance of observations.

Moreover, the work with the NCAR large ensemble focuses on future evolution of heat transport to the Arctic. This is a state-of-the-art ensemble and the results can be compared with previous studies on transport to the Barents and Kara Seas at higher CO_2 levels. It will lead to a better insight in model dependency on the role of heat transport on Arctic change.

Additionally, the MPI-ESM Grand Ensemble (MPI-GE) is the largest ensemble available. Further, the ocean is also initialised in this large ensemble, which makes it unique, especially for studying the forced

changes in the ocean heat transport and to disentangle the forced change from internal ocean variability.

Finally, the coupled model sensitivity experiments are unique and give insight in the fundamentals of the coupled climate system, in particular the coupling between atmosphere and ocean and the impact of orography on meridional heat transport.

All these studies address the impact of meridional energy transport on Arctic climate and Arctic amplification.

Impact

How has this work contributed to the expected impacts of Blue-Action?

All the studies mentioned above address the impact of meridional heat transport on the Arctic. The scientific impact is clear, based on the peer reviewed publications that are based on these studies. There is an ongoing debate on the role of regional feedbacks and remote processes and these studies contribute to this scientific question.

The studies show that it is crucial to improve monitoring of the atmosphere and ocean to constrain variations in meridional heat transport. The current observational systems are insufficient to constrain the transports.

The wider impact of the studies address the understanding of Arctic change, in particular the rapid warming in the region and the associated reduction of sea ice and snow. The region is politically and economically of interest and ecologically vulnerable.

The studies contribute to the reliability of estimates of the projected future Arctic change and to improved weather forecast studies. The studies show that improved process description is necessary to improve weather and climate predictions for the region. This includes the representation of ocean processes (heat uptake and heat transport in key regions) and atmospheric processes (e.g. the storm tracks, standing eddies, impact of orography).

The studies indicate the complexity and that remote processes must be taken into account, that is, Arctic change does not stand on its own, but is an integral part of the changes in the global climate changes, where changes in the Atlantic ocean and in the atmospheric circulation affect the Arctic.

Impact on the business sector

The outcome from this project will help to improve the sea ice predictions in the Arctic region, which would contribute to the safety and sustainability of shipping industry. This is relevant for the Blue-Action case study 3 Extreme weather risks to maritime activities http://www.blue-action.eu/index.php?id=4144&L=0%2Fwp-login.php%3F9%3D9c9216

Lessons learned and Links built

This study shows that all selected reanalyses data sets agree on the mean northward heat transport in the Northern Hemisphere. The results are consistent with those achieved over the previous 20 years (Trenberth and Caron, 2001; Fasullo and Trenberth, 2008; Mayer and Haimberger, 2012).

However, atmospheric and oceanic heat transport anomalies at interannual time scales they differ from each other, both spatially and temporally. Although there is an overlap of observational data assimilated by different reanalyses products, large deviations still exist in main fields, especially for the vertical profiles of temperature and velocity in atmospheric reanalyses. As a consequence, much care should be taken when adopting the reanalyses for investigations on energy balance and energy transport related issues, especially for the ones aiming at relatively large time scales.

In order to improve the accuracy of variability of AMET and OMET estimated from reanalyses, we need more observations to constrain the models. This is of direct relevance to observational programs such as INTAROS and there are active discussions between consortium members of the programs.

The outcomes of this study can provide more insight to APPLICATE and PRIMAVERA, which attempt to improve the skills in weather and climate prediction, too. In particular high resolution climate models developed in PRIMAVERA can be better assessed with these results and it is clear in which direction the models need to improve. The same models will be used in APPLICATE for predictions.

Contribution to the top level objectives of Blue-Action

Objective 1 Improving long range forecast skill for hazardous weather and climate events

Improved understanding of estimates of past changes that are used to assess forecast skill (e.g. the quality of reanalyses products).

Improved process descriptions and resolution in coupled weather and climate models.

Objective 2 Enhancing the predictive capacity beyond seasons in the Arctic and the Northern Hemisphere

The work gives insight in the relevant processes that will need to be improved to increase the predictive capacity. Heat transport on interannual to decadal time scales is considered. This fundamental property of the climate system is better understood now which will aid in enhancing predictive capacity.

Objective 3 Quantifying the impact of recent rapid changes in the Arctic on Northern Hemisphere climate and weather extremes

Meridional ocean and atmospheric heat transport is quantified in the historical period. The eddy heat transport (both standing and transient) is shown to be important and strongly related to storms and

blocking (hence cold and warm spells).

Objective 4 Improving the description of key processes controlling the impact of the polar amplification of global warming in prediction systems

By quantifying heat transport in the atmosphere and ocean, and providing more insights on the relation between variability of northward heat transport and prediction of the Arctic weather and climate.

Objective 5 Optimizing observational systems for predictions

By emphasizing the importance of independent observations in the ocean to validation and verification of climate models and weather predictions.

Objective 6 Reducing and evaluating the uncertainty in prediction systems

Epistemic uncertainty is reduced by better understanding of the processes. Also, a better understanding of the spread in the reanalyses data sets aids in reducing, or at least quantifying, uncertainty.

Objective 7 Fostering the capacity of key stakeholders to adapt and respond to climate change and boosting their economic growth

The objective is indirectly contributed to through the aspects mentioned above.

Objective 8 Transferring knowledge to a wide range of interested key stakeholders

The objective is indirectly contributed to through the aspects mentioned above.

References (Bibliography)

- Balmaseda, M. A., Mogensen, K., and Weaver, A. T.: Evaluation of the ECMWF ocean reanalyses system ORAS4, Quarterly Journal of the Royal Meteorological Society, 139, 1132–1161, 2013.
- Carton, J. A., Chepurin, G. A., and Chen, L.: SODA3: a new ocean climate reanalyses, Journal of Climate, 2018.
- Dee, D. P., Uppala, S. M., Simmons, A., Berrisford, P., Poli, P., Kobayashi, S., Andrae, U., Balmaseda, M., Balsamo, G., Bauer, d. P., et al.: The ERA-Interim reanalyses: Configuration and performance of the data assimilation system, Quarterly Journal of the royal meteorological society, 137, 553–597, 2011.
- Dufour, A., Zolina, O., and Gulev, S. K.: Atmospheric moisture transport to the Arctic: Assessment of reanalyses and analysis of transport components, Journal of Climate, 29, 5061–5081, 2016.
- Fasullo, J. T. and Trenberth, K. E.: The annual cycle of the energy budget. Part II: Meridional structures and poleward transports, Journal of Climate, 21, 2313–2325, 2008.

- Ferry, N., Parent, 5 L., Garric, G., Barnier, B., Jourdain, N. C., et al.: Mercator global Eddy permitting ocean reanalyses GLORYS1V1: Description and results, Mercator-Ocean Quarterly Newsletter, 36, 15–27, 2010.
- Ferry, N., Parent, L., Garric, G., Bricaud, C., Testut, C., Le Galloudec, O., Lellouche, J., Drevillon, M., Greiner, E., Barnier, B., et al.: GLORYS2V1 global ocean reanalyses of the altimetric era (1992–2009) at meso scale, Mercator Ocean–Quaterly Newsletter, 44, 2012b.
- Fleming, L.E., Y.-O. Kwon, R. Vargas-Martes, G. Gebbie, and H. Furey: The Influence of Northward
- Heat Transport on Arctic Amplification in the Community Earth System Model Version 1 Large Ensemble. Geophys. Res. Lett., 2019, Submitted.
- Gelaro, R., McCarty, W., Suárez, M. J., Todling, R., Molod, A., Takacs, L., Randles, C. A., Darmenov, A., Bosilovich, M. G., Reichle, R., et al.: The modern-era retrospective analysis for research and applications, version 2 (MERRA-2), Journal of Climate, 30, 5419–5454, 2017
- Gent, P. R. and Mcwilliams, J. C.: Isopycnal mixing in ocean circulation models, Journal of Physical Oceanography, 20, 150–155, 1990.
- Graversen, R. G., Källén, E., Tjernström, M., and Körnich, H.: Atmospheric mass-transport inconsistencies in the ERA-40 reanalyses, Quarterly Journal of the Royal Meteorological Society, 133, 673–680, 2007.
- Graversen, R. G., Mauritsen, T., Tjernström, M., Källén, E., and Svensson, G.: Vertical structure of recent Arctic warming, Nature, 451, 53, 2008.
- Hall, M. M. and Bryden, H. L.: Direct estimates and mechanisms of ocean heat transport, Deep Sea Research Part A. Oceanographic Research Papers, 29, 339–359, 1982.
- Harada, Y., Kamahori, H., Kobayashi, C., Endo, H., Kobayashi, S., Ota, Y., Onoda, H., Onogi, K., Miyaoka, K., and Takahashi, K.: The JRA-55 reanalyses: Representation of atmospheric circulation and climate variability, Journal of the Meteorological Society of Japan. Ser. II, 94, 269–302, 2016.
- Johns, W. E., Baringer, M. O., Beal, L. M., Cunningham, S., Kanzow, T., Bryden, H. L., Hirschi, J., Marotzke, J., Meinen, C., Shaw, B.,et al.: Continuous, array-based estimates of Atlantic Ocean heat transport at 26.5 N, Journal of Climate, 24, 2429–2449, 2011.
- Jungclaus, J.H., K. Lohmann, and D. Zanchettin, 2014: Enhanced 20th century heat transfer to the Arctic simulated in the context of climate variations over the last millennium. Climate of the Past, 10, 2201-2213, doi:10.5194/cp-10-2201-2014.
- Kobayashi, S., Ota, Y., Harada, Y., Ebita, A., Moriya, M., Onoda, H., Onogi, K., Kamahori, H., Kobayashi, C., Endo, H., et al.: The JRA-55 reanalyses: General specifications and basic characteristics, Journal of the Meteorological Society of Japan. Ser. II, 93, 5–48, 2015.
- Lott, F., & Miller, M. J.: A new subgrid-scale orographic drag parametrization: Its formulation and testing. Quarterly Journal of the Royal Meteorological Society, 123(537), 101-127, 1997.
- Lott, F.: Alleviation of stationary biases in a GCM through a mountain drag parameterization scheme and a simple representation of mountain lift forces. Monthly weather review, 127(5), 788-801, 1999.
- Lozier, M., Li, F., Bacon, S., Bahr, F., Bower, A., Cunningham, S., de Jong, M., de Steur, L., Fischer, J., Gary, S., et al.: A sea change in our view of overturning in the subpolar North Atlantic, Science, 363, 516–521, 2019.
- Madec, G.: NEMO reference manual, ocean dynamic component: NEMO-OPA, Note du Pôle modélisation, Inst. Pierre Simon Laplace, Fr, 2008.

- Maher, N. et al. The Max Planck Institute Grand Ensemble Enabling the Exploration of Climate System Variability. Journal of Advances in Modeling Earth Systems (2019).
- Marzocchi, A., Hirschi, J. J.-M., Holliday, N. P., Cunningham, S. A., Blaker, A. T., and Coward, A. C.: The North Atlantic subpolar circulation in an eddy-resolving global ocean model, Journal of Marine Systems, 142, 126–143, 2015.
- Masina, S., Storto, A., Ferry, N., Valdivieso, M., Haines, K., Balmaseda, M., Zuo, H., Drevillon, M., and Parent, L.: An ensemble of eddy permitting global ocean reanalyses from the MyOcean project, Climate Dynamics, 49, 813–841, 2017.
- Mayer, M. and Haimberger, L.: Poleward atmospheric energy transports and their variability as evaluated from ECMWF reanalyses data, Journal of Climate, 25, 734–752, 2012.
- Mayer, M., Haimberger, L., Edwards, J. M., and Hyder, P.: Toward consistent diagnostics of the coupled atmosphere and ocean energy budgets, Journal of Climate, 30, 9225–9246, 2017.
- McCarthy, G., Smeed, D., Johns, W., Frajka-Williams, E., Moat, B., Rayner, D., Baringer, M., Meinen, C., Collins, J., and Bryden, H.: Measuring the Atlantic meridional overturning circulation at 26 N, Progress in Oceanography, 130, 91–111, 2015.
- Moat, B., Josey, S., Sinha, B., Blaker, A., Smeed, D., McCarthy, G., Johns, W., Hirschi, J.-M., Frajka-Williams, E., Rayner, D., et al.: Major variations in subtropical North Atlantic heat transport at short (5 day) timescales and their causes, Journal of Geophysical Research: Oceans, 121, 3237–3249, 2016.
- Riser, S. C., Freeland, H. J., Roemmich, D., Wijffels, S., Troisi, A., Belbéoch, M., Gilbert, D., Xu, J., Pouliquen, S., Thresher, A., et al.:Fifteen years of ocean observations with the global Argo array, Nature Climate Change, 6, 145, 2016.
- Roberts, M. J., Baker, A., Blockley, W., Calvert, D., Coward, A., Hewitt, H. T., ... & Schiemann, R. Description of the resolution hierarchy of the global coupled HadGEM3-GC3. 1 model as used in CMIP6 HighResMIP experiments.
- Sandu, I., van Niekerk, A., Shepherd, T. G., Vosper, S. B., Zadra, A., Bacmeister, J., ... & Pithan, F: Impacts of orography on large-scale atmospheric circulation. npj Climate and Atmospheric Science, 2(1), 10., 2019
- Stepanov, V. and Haines, K.: Mechanisms for AMOC variability simulated by the NEMO model, Ocean Science, 10, 645–656, 2014.
- Susan Lozier, M., Bacon, S., Bower, A. S., Cunningham, S. A., Femke de Jong, M., De Steur, L., deYoung, B., Fischer, J., Gary, S. F., Greenan, B. J., et al.: Overturning in the Subpolar North Atlantic Program: A new international ocean observing system, Bulletin of the American Meteorological Society, 98, 737–752, 2017.
- Trenberth, K. E.: Climate diagnostics from global analyses: Conservation of mass in ECMWF analyses, Journal of Climate, 4, 707–722, 1991.
- Trenberth, K. E. and Caron, J. M.: Estimates of meridional atmosphere and ocean heat transports, Journal of Climate, 14, 3433–3443, 2001.
- Trenberth, K. E., Stepaniak, D. P., and Caron, J. M.: Accuracy of atmospheric energy budgets from analyses, Journal of Climate, 15, 3343–3360, 2002.
- Zheng, Y. and Giese, B. S.: Ocean heat transport in simple ocean data assimilation: Structure and mechanisms, Journal of Geophysical Research: Oceans, 114, 2009.

Dissemination and exploitation of Blue-Action results

Dissemination activities

Type of dissemination activity	Name of the scientist (institution), title of the presentation, event	Place and date of the event	Type of Audience	Estimated number of persons reached	Link to Zenodo upload
Participation to a conference	Yang Liu (NLeSC), talk title: Meridional Energy Transport from Midlatitudes towards the Arctic, at EGU 2018	Vienna (AT), 9 – 13 April 2018	Scientific Community (higher education, Research)	100	https://zenodo.org/record/1219722#.XVq27ugzZGM
Participation to a workshop	Yang Liu (NLeSC), **talk t**itle: Synthesis and Evaluation of Meridional Heat Transport from Mid-latitudes towards the Arctic, at EEI 2018	Toulouse (FR), 13-16 November 2018	Scientific Community (higher education, Research)	60	https://zenodo.org/record/1492297#.XVq4GOgzZGM
Participation to a conference	Rohit Ghosh (MPI-M), talk title: Nonlinear changes in the North Atlantic Ocean circulations under global warming, at AGU 2018	Washington (US), 10-14 December 2018	Scientific Community (higher education, Research)	50	https://www.zenodo.org/communities/blue-actionh2020/
Participation to a conference	Rohit Ghosh (MPI-M), talk title: Two distinct phases of North Atlantic gyre circulation changes under global warming, at EGU 2019	Vienna (AT), 7-12 April 2019	Scientific Community (higher education, Research)	100	https://www.zenodo.org/communities/blue-actionh2020/

Other publications

These are the publications currently in review or submitted:

Under review

- Synthesis and evaluation of historical meridional heat transport from midlatitudes towards the Arctic, Y.Liu, B. Moat, J. J. Attema, W. Hazeleger, Earth System Dynamics.
- Atmosphere-ocean interactions and their footprint on heat transport variability in the Northern Hemisphere, Y.Liu, J. J. Attema, W. Hazelege, Journal of Climate.

- The Influence of Northward Heat Transport on Arctic Amplification in the Community Earth System Model Version 1 Large Ensemble, Fleming, L.E., Y.-O. Kwon, R. Vargas-Martes, G. Gebbie, and H. Furey, Geophysical Research Letter.

Submitted:

- North Atlantic Gyres evolve in two distinct phases under global warming, R. Ghosh, D. Putrasahan, E. Manzini, D. Matei et.al.

Uptake by the targeted audiences

As indicated in the Description of the Action, the audience for this deliverable is the general public (PU) is and is made available to the world via CORDIS.

This is how we are going to ensure the uptake of the deliverables by the targeted audiences:

- Through dissemination at relevant scientific events (AGU, EGU…).
- Through dissemination to relevant non scientific audiences, such as civil society, businesses and policy makers: see D8.8 Societal Engagement Knowledge Exchange Nr. 2, on Ocean observations and predictions in response to the climate emergency.